LCLS-II Technical Note

Optics for R56 tuning in the LCLS-II

LCLS-II-TN-23-01

1/12/2023

Y. Nosochkov

1 Introduction

R_{56} is a first order matrix term describing transformation of particle longitudinal position (z) in a bunch as a function of particle relative momentum deviation (δ):

$$z_f = z_i + R_{56}\delta_i \tag{1}$$

Here, i and f denote the initial and final particle positions when transported through a beamline section, $\delta = \frac{p-p_0}{p_0}$ is the relative momentum deviation, where p and p_0 are the particle momentum and the design momentum, respectively.

The primary sources of R_{56} are dipoles, where particle orbits are momentum dependent. The R_{56} can be expressed through the dispersion function (η) and the dipole bending radius (ρ) or the bending angle (θ):

$$R_{56} = \int \frac{\eta}{\rho} ds = \sum_k \langle \eta_k \rangle \theta_k \tag{2}$$

where $\langle \eta \rangle$ is an average dispersion in a dipole. Sign convention for η, ρ, θ in Eq. (2) is the same as defined in MAD [1]. However, the sign of R_{56} in Eq. (2) and elsewhere in this note is opposite to the one in MAD. With this convention, the R_{56} produced by a closed orbit bump bending system without inner quadrupoles is always negative.

Here, we ignore the contribution to the R_{56} from the energy dependent term, $-\frac{L}{\beta^2\gamma^2}$, where L is the length of a beamline section, and β, γ are Lorenz factors, because it is negligible at the GeV beam energies considered here.

Ability to tune R_{56} in the LCLS-II [2] is critical for optimization of bunch length (e.g., for producing short pulses), maximizing peak current, and mitigating micro-bunching instability. Most of the LCLS-II R_{56} tuning sections reside in the beginning of the machine; these include the Laser Heater [3] chicane and the BC1 [4], BC2 [5] bunch compressor chicanes. The downstream regions have special R_{56} compensating chicanes [6] positioned next to main dipoles. The latter chicanes are adequate for compensation of the dipole R_{56} and suppression of the micro-bunching instability [7], but may be too weak for other beam manipulation tasks. One limitation of the LCLS-II chicanes is that they produce only negative R_{56}. However, according to the ongoing beam shaping studies, there is also the need for positive R_{56} adjustment in the range of a few mm [8]. In addition, the shaping studies call for the need of R_{56} tuning optics closer to the undulator area.

Here, we present one design of a dedicated optics for R_{56} tuning in the LCLS-II. Note that this optics is not part of the nominal LCLS-II. Some of the key features of this design are:

- Four-dipole chicane with inner quadrupoles and sextupoles
- R_{56} tuning range from -2 mm to +8 mm
- Beam energy up to 8.5 GeV, adequate for LCLS-II and suitable for LCLS-II-HE
- Based on the LCLS-II type magnet designs
- Fixed layout does not require magnet movers
- Positions of the nominal LCLS-II magnets and devices are not affected
- The R_{56} optics can be turned off for the nominal LCLS-II operation mode
- Chicane dispersion is cancelled to second order for minimal emittance growth

2 Optics design

The R_{56} optics must contain dipoles as follows from Eq. (2). The latter create beam trajectory different from the nominal beam path. The requirement that the positions of the nominal LCLS-II beamline elements must not be affected leads to the following considerations:

- The R_{56} optics layout must be of a closed bump design such as a chicane
- The new magnets must be sufficiently separated from the existing LCLS-II magnets and devices

- A free space of a sufficient length in the nominal LCLS-II is required to accommodate such optics

We choose a design based on a symmetric four-dipole chicane. As noted earlier, a chicane made of only dipoles creates negative R_{56}. This is due to the negative sign of the dominant terms $\eta\theta$ in Eq. (2), created by the inner dipoles. In order to obtain a positive sign of the R_{56}, dispersion in the inner dipoles must be either sufficiently suppressed or forced to change sign. This can be realized by adding quadrupoles inside the chicane. When properly positioned, the quadrupoles can provide the required focusing of the dispersion at the inner dipoles. Furthermore, the quadrupole focusing can be varied to produce variation of the dispersion for R_{56} tuning. Note that the small dispersion in the outer chicane dipoles is determined by the condition of dispersion cancellation at each end of the chicane, and therefore is not affected by the R_{56} tuning.

Insertion of the R_{56} optics into the LCLS-II must not alter the nominal magnet layout; hence, compatible locations must be drifts of sufficient length. The more compact the chicane, the better chances for finding suitable locations for such optics. Main factors affecting the minimum chicane length are:

- Maximum beam energy
- Maximum achievable magnet strengths
- Required separation between the chicane magnets and the nominal LCLS-II beamline to avoid interference
- Adequate spacing between quadrupoles for efficient focusing

In this design, the chicane length, from the beginning of the first dipole to the end of the last dipole, is 45 m. The symmetric chicane is not automatically matched to the LCLS-II optics. Hence, additional quadrupoles may be needed outside of the chicane for matching, thus, demanding for more space. Sufficiently long drift sections exist only in the LCLS-II bypass line with ~100 m spacing between quadrupoles. We choose the last long drift of the bypass in order to position the R_{56} optics as close as possible to the undulators. This location, however, is still upstream of the beam spreader, hence the R_{56} tuning in this optics would equally affect bunches going to either undulator.

The complete LCLS-II layout and the nominal LCLS-II-HXR optics are shown in Figure 1 and Figure 2, respectively, where the selected chicane location is indicated by arrow. Figure 3 shows the nominal optics functions at this location (without R_{56} optics).

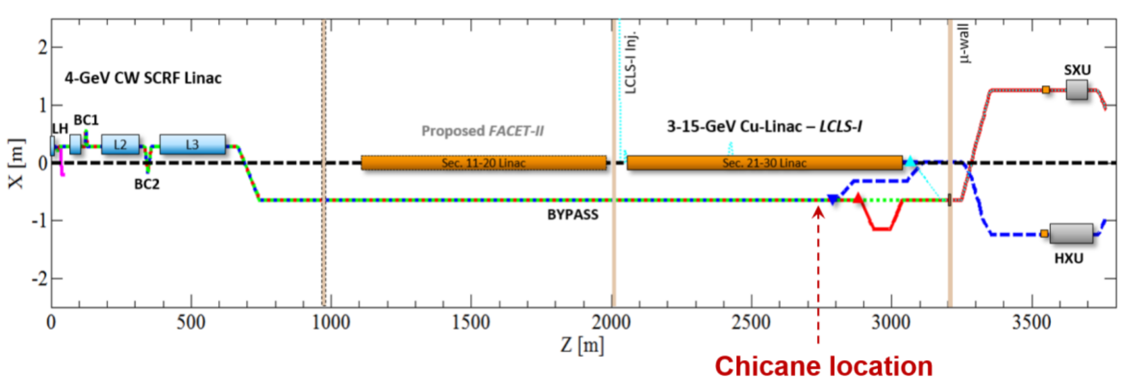

Figure 1: Top view layout of the LCLS-II and selected location of the R_{56} chicane in this study.

The designed R_{56} optics is inserted in the last long drift of the bypass. The R_{56} layout in this section is shown in Figure 4. The optics consists of the 45-m long chicane and several matching quadrupoles outside of the chicane. Two operational beam modes are possible. When all the R_{56} magnets are turned off, the beam follows the nominal beam path, and the nominal LCLS-II optics is used. When the R_{56} optics is turned on, the beam travels through the chicane, and the magnet strengths are set for desired R_{56}.

The chicane magnets include four identical rectangular dipoles, six quadrupoles, and four sextupoles. The chicane is mirror symmetric with respect to its center, both in terms of magnet positions and their strengths. The dipole bending angles are fixed, regardless of the R_{56} setting, to avoid the need for potentially complicated and expensive mover system. The dipoles are yawed at half bending angle for a minimal sagitta. Beam trajectory in the chicane is 18.29 mm longer than in the nominal LCLS-II straight line, thus producing 61 ps delay compared to the nominal optics.

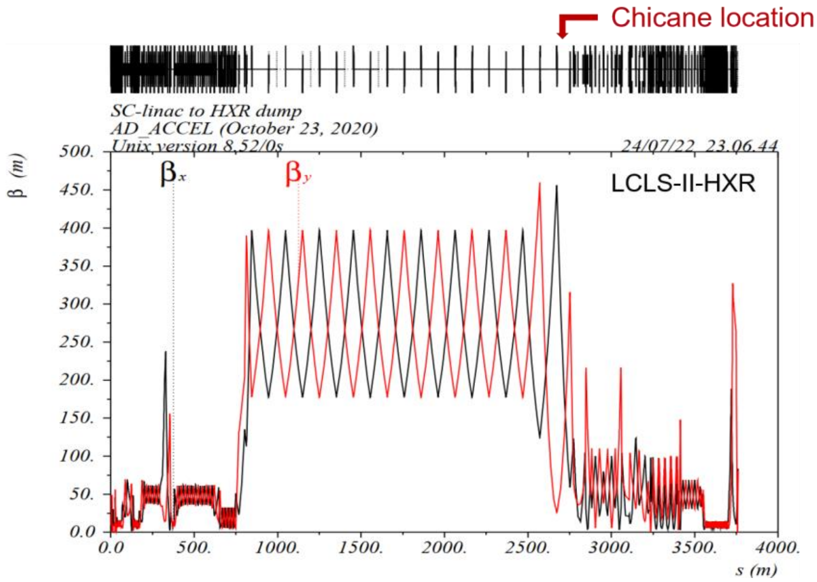

Figure 2: LCLS-II nominal beta functions from injector to HXR dump. The arrow points at the selected location of the R_{56} chicane.

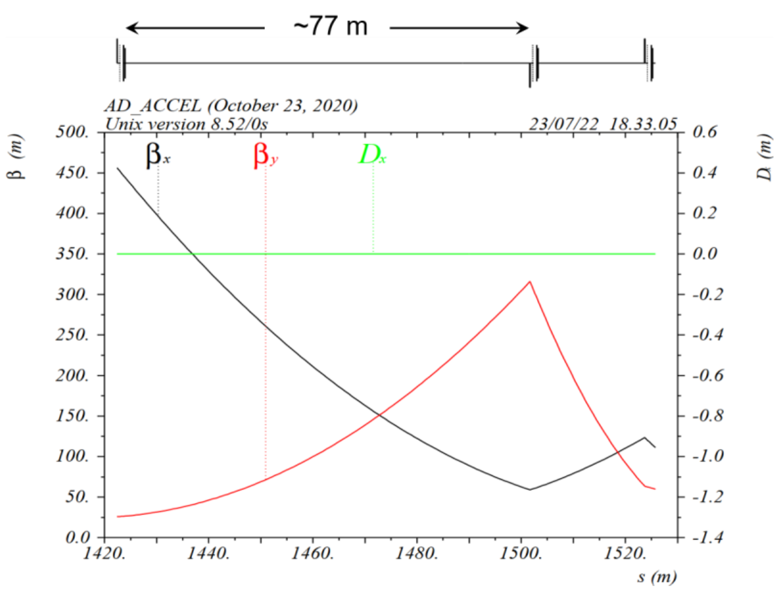

Figure 3: Nominal optics functions in the last bypass section, without the R_{56} chicane.

An important consideration is the choice of the bending angle values and magnet positions. To keep the system compact and avoid interference with the existing LCLS-II line, a near maximum bending angle is used (32 mrad) as allowed by the dipole field at up to 8.5 GeV beam energy, while the inner chicane magnets are placed at locations where the horizontal offset is sufficiently large. The smallest magnet separation from the nominal LCLS-II line is at the first and the last chicane quadrupoles, where the offset is 357 mm; the latter should be sufficient for the magnet installation without interference. The maximum offset is 582 mm at the magnets in the middle of the chicane.

The chicane's primary function is to tune the R_{56}. The match to the nominal LCLS-II beta functions is achieved by using additional seven quadrupoles inserted in the same drift outside of the chicane. Finally, four sextupoles are included for cancellation of the chicane second order dispersion. For cost effective solution, all the new magnets of the R_{56} optics are of the existing LCLS-II designs. Parameters of the magnets and their survey coordinates in the SLAC linac coordinate system are shown in Table 1.

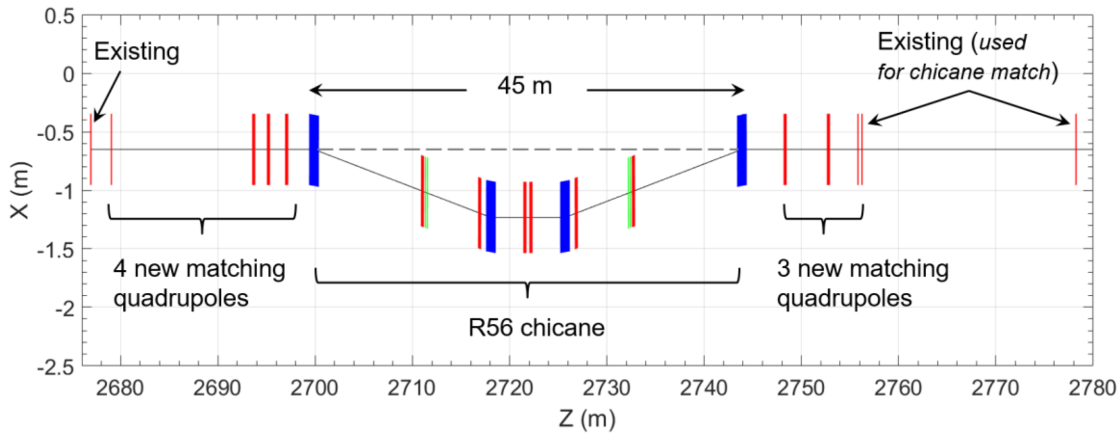

Figure 4: Top view layout of the last bypass section with the inserted R_{56} chicane and additional matching quadrupoles, where dipoles are shown in blue color, quadrupoles are in red, and sextupoles in green.

Table 1: Parameters of the new magnets in the R_{56} optics and the survey coordinates at the magnet centers in the SLAC linac coordinate system. Quadrupoles are shown in black color, dipoles are in red, and sextupoles are in blue. *(* Dipole coordinates correspond to the center of beam trajectory and not to the physical magnet center)*

Name	Type	Effective Length, m	Bore Radius / Half Gap, mm	X, m	Y, m	Z, m
QBP37	2Q4W	0.1244	26.9	-0.650494	0.649478	2679.038203
QBP38	1.26Q12	0.32	16.0	-0.650494	0.649478	2693.678085
QBP39	1.26Q12	0.32	16.0	-0.650494	0.649478	2695.198085
QBP40	1.26Q12	0.32	16.0	-0.650494	0.649478	2697.068085
BCXBP1	1.0D38.37	1.0	12.7	-0.654494	0.649478	2699.878085
QBCBP1	1.26Q12	0.32	16.0	-1.007555	0.649478	2711.032499
SBCBP1A	1.38S3.00	0.1	17.5	-1.017473	0.649478	2711.342341
SBCBP1B	1.38S3.00	0.1	17.5	-1.023872	0.649478	2711.542238
QBCBP2	1.26Q12	0.32	16.0	-1.195680	0.649478	2716.909404
BCXBP2	1.0D38.37	1.0	12.7	-1.228796	0.649478	2718.068938
QBCBP3	1.26Q12	0.32	16.0	-1.232796	0.649478	2721.568085
QBCBP4	1.26Q12	0.32	16.0	-1.232796	0.649478	2722.188085
BCXBP3	1.0D38.37	1.0	12.7	-1.228796	0.649478	2725.687232
QBCBP5	1.26Q12	0.32	16.0	-1.195680	0.649478	2726.846766
SBCBP2A	1.38S3.00	0.1	17.5	-1.023872	0.649478	2732.213931
SBCBP2B	1.38S3.00	0.1	17.5	-1.017473	0.649478	2732.413829
QBCBP6	1.26Q12	0.32	16.0	-1.007555	0.649478	2732.723670
BCXBP4	1.0D38.37	1.0	12.7	-0.654494	0.649478	2743.878085
QBP41	1.26Q12	0.32	16.0	-0.650494	0.649478	2748.328085
QBP42	1.26Q12	0.32	16.0	-0.650494	0.649478	2752.778085
QBP43	2Q4W	0.1244	26.9	-0.650494	0.649478	2755.806903

The sign of the chicane bending angles is chosen somewhat arbitrarily, producing the trajectory offset to the South. However, this optics works equally well for the reversed sign of the bending angles. The latter will change the sign of the beam trajectory, moving it to the North side. This will not affect the focusing and the beta functions. The linear dispersion will change sign, but will remain cancelled. The second order dispersion will be also cancelled by simply changing the sign of the sextupole strengths.

The chicane optics is optimized independently of its location in the LCLS-II. The magnets (four dipoles, six quadrupoles, and four sextupoles) are positioned symmetrically relative to the chicane center. The latter allows us to create symmetric optics, where pairs of the mirror symmetric magnets have the same strength. In this case, the six quadrupoles are grouped into three families, and the four sextupoles into one family. The quadrupole positions are optimized to produce minimum beta functions, while providing cancellation of the linear dispersion, for any R_{56} setting. Due to the symmetric design, the chicane beta functions are chosen to be symmetric relative to the chicane center as well. The latter, however, is not a requirement; the beta functions in the chicane can be changed, if needed, by the outside matching quadrupoles without affecting the chicane dispersion and the R_{56}.

To minimize the chromatic emittance growth, the chicane second order dispersion is cancelled using symmetrically located sextupoles. The existing LCLS-II type sextupoles are used for cost saving. However, due to limited strength, two of such sextupoles are needed next to each of the first and the last chicane quadrupoles, for total of four sextupoles. They are arranged in one family.

Tuning of the R_{56} is realized by adjustment of the linear dispersion at the inner dipoles to the necessary level in accordance with Eq. (2). The latter is performed by the chicane quadrupoles fitting the dispersion while maintaining reasonable beta functions. The achieved variation of the R_{56} is from -2 mm to +8 mm which is within the desired range for beam shaping. The chicane sextupole strengths are also adjusted with the R_{56} in order to maintain cancellation of the second order dispersion.

The tuning range is limited by the rapidly increasing beta functions at large negative R_{56} values, and by Beam Stay Clear (BSC) in the chicane center quadrupoles at large positive R_{56} due to growth of linear dispersion. The chicane optics functions are optimized within the tuning range at multiple points with a step of ΔR_{56} = 1 mm. As an example, Figure 5 and Figure 6 show the optimized beta functions, and the first and the second order dispersion, respectively, at four R_{56} points: -2 mm, 0, +5 mm, and +8 mm. One can see that the peak beta functions grow as R_{56} is decreasing, and the peak absolute dispersion grows when R_{56} is increasing, thus limiting the tuning range.

The chicane optimized symmetric beta functions are matched to the existing beta functions in the bypass using matching quadrupoles outside of the chicane. These include the new seven matching quadrupoles and two existing LCLS-II quadrupoles as shown in Figure 4, which are arranged in eight families. The match is done for the entire R_{56} range with a step of ΔR_{56} = 1 mm. Figure 7 shows examples of the matched optics functions within the last bypass section at the four R_{56} points: -2 mm, 0, +5 mm, and +8 mm.

Horizontal and vertical Beam Stay Clear in the R_{56} magnets is determined based on the LCLS-II definition [9], where the half-width BSC is:

$$BSC = 16\sqrt{2\beta\varepsilon} + 1.25|\eta|\delta + \Delta x \tag{3}$$

Here, the conservative normalized emittance is $\gamma\varepsilon$ = 1 μm where γ is the Lorenz factor at 4 GeV, δ = 2.05% is the maximum possible half-width of energy spread in the bypass, Δx = 2 mm is the maximum steering error, and β and η are the beta function and linear dispersion in the corresponding plane. The resulting horizontal and vertical BSC in the bypass section, where the R_{56} optics is inserted, are shown in Figure 8 at four R_{56} points: -2 mm, 0, +5 mm, and +8 mm. The BSC satisfies the magnet apertures, listed in Table 1, for the entire R_{56} tuning range. The horizontal BSC limits the maximum positive R_{56} value to +8 mm due to the increasing dispersion in the chicane center quadrupoles when the R_{56} is increasing, as can be seen in Figure 6.

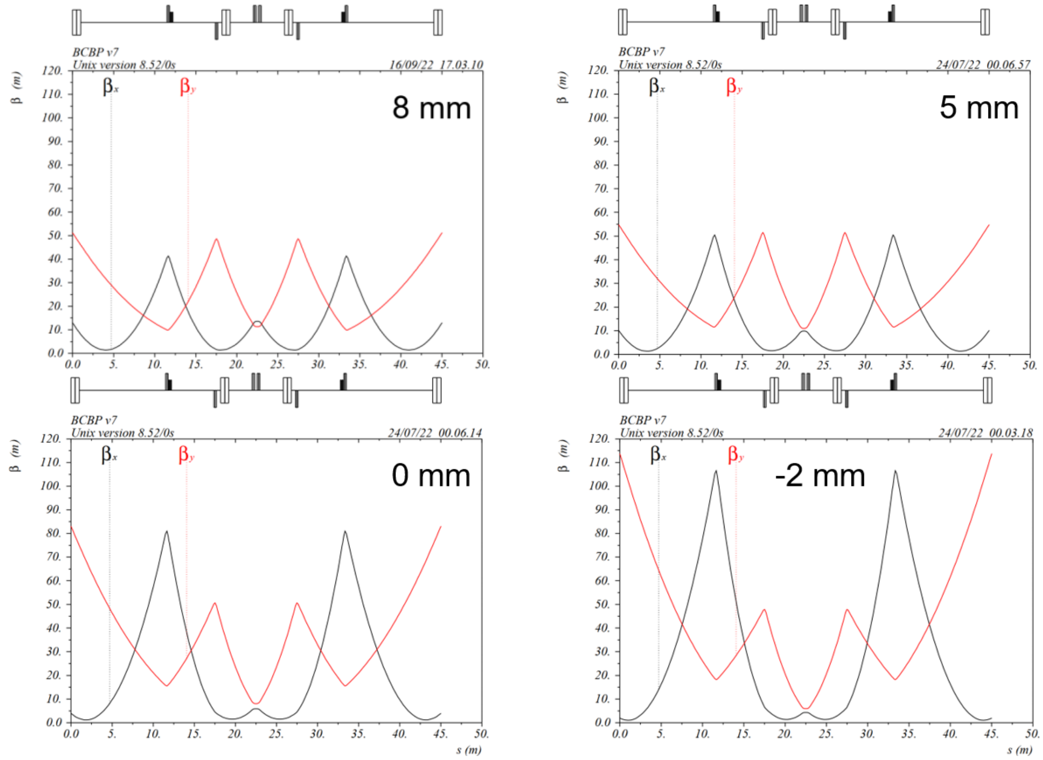

Figure 5: Optimized beta functions in the R_{56} chicane for R_{56} = -2 mm, 0, 5 mm, and 8 mm.

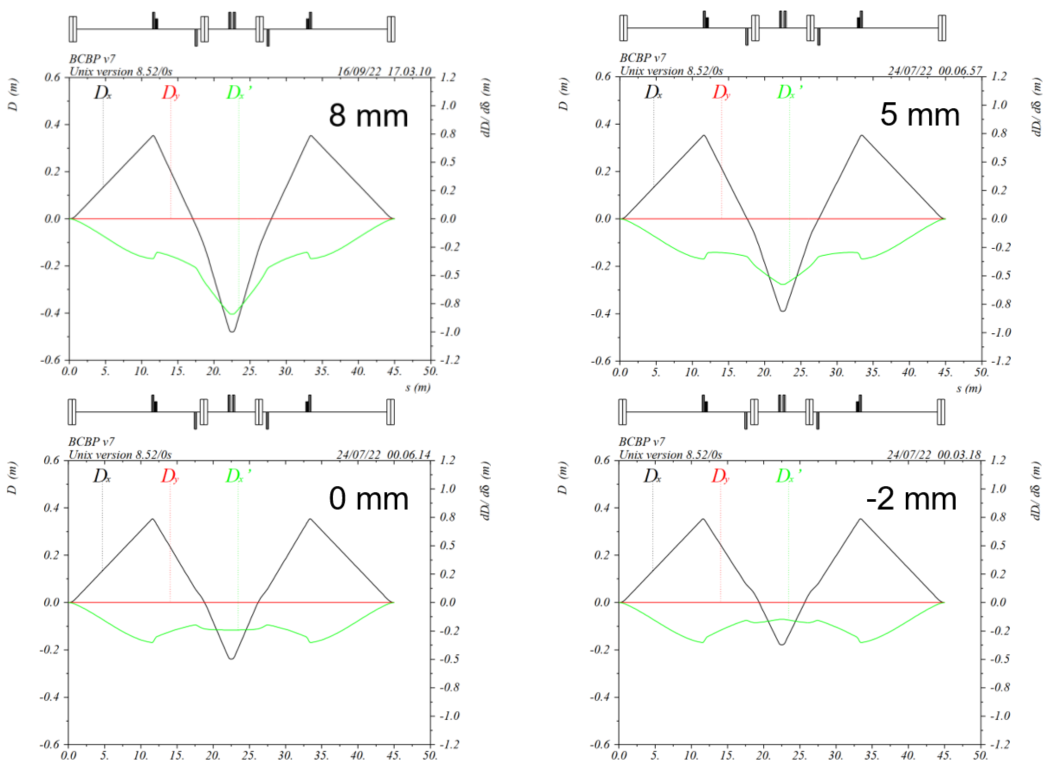

Figure 6: First and second order dispersion in the R_{56} chicane for R_{56} = -2 mm, 0, 5 mm, and 8 mm.

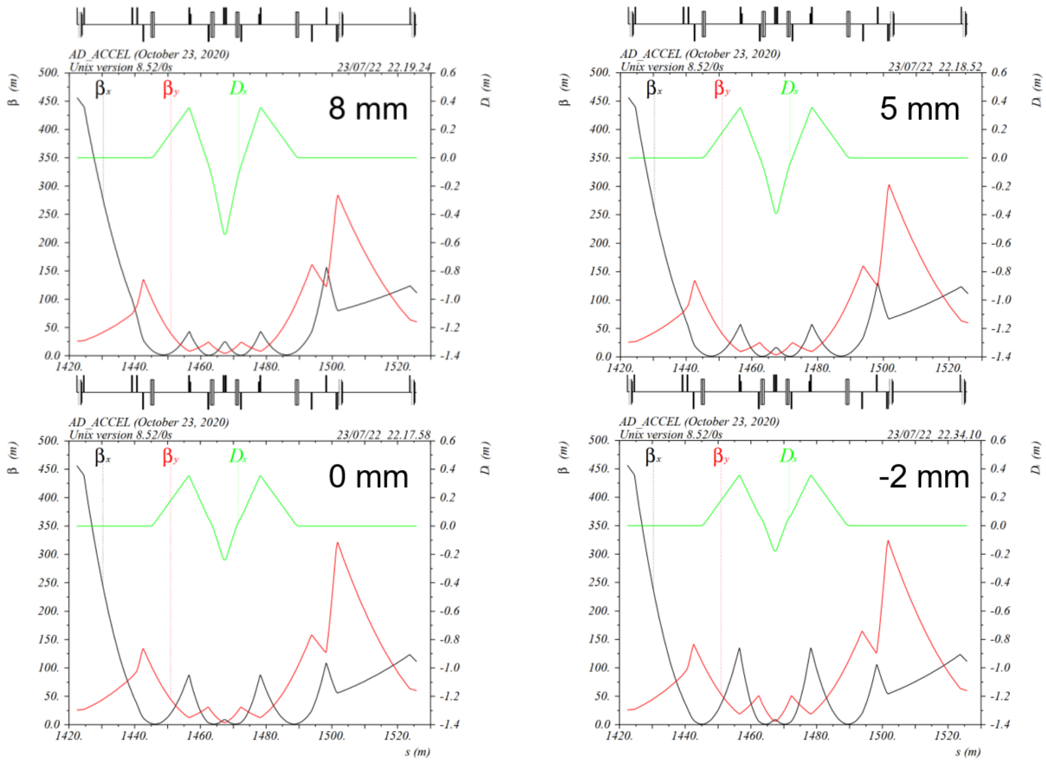

Figure 7: Matched optics functions in the bypass section with the R_{56} chicane for R_{56} = -2 mm, 0, 5 mm, and 8 mm.

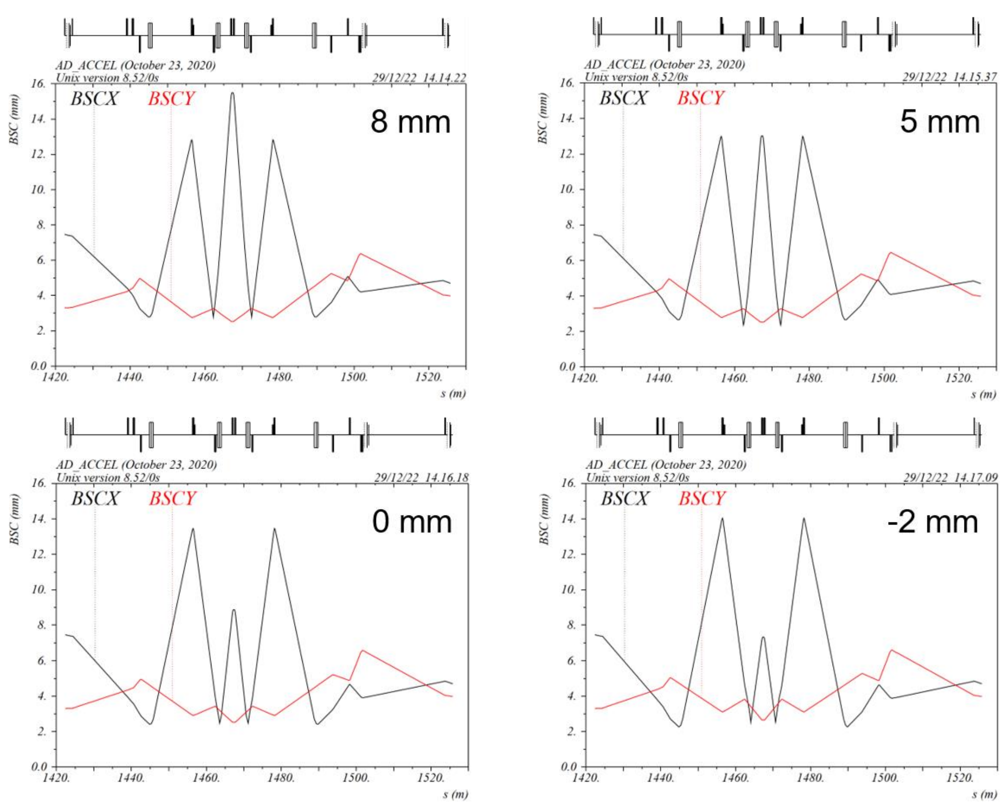

Figure 8: Horizontal (black) and vertical (red) Beam Stay Clear in the bypass section with the R_{56} optics for R_{56} = -2 mm, 0, 5 mm, and 8 mm.

The described R_{56} tuning optics is based on the four-dipole chicane designed to be used with the inner quadrupoles and sextupoles, and the outside matching quadrupoles. However, there is one special case of this optics where all the new magnets are turned off, except the dipoles, and the existing LCLS-II quadrupoles are at their nominal strengths. In this configuration, the optics reduces to a simple four-dipole chicane producing the same trajectory as in the original R_{56} optics. The focusing effect from the chicane dipoles is very small, therefore the nominal LCLS-II beta functions are practically not affected and do not require a re-match. The chicane linear and second order dispersion are also cancelled. Therefore, such configuration is also optically matched to the LCLS-II. This quadrupole-free chicane has a large negative R_{56} = -36.6 mm. The latter appears to be too far outside of the desired range for beam shaping. More importantly, it is not tunable since the dipole angles are fixed. For such a simple chicane, the second order term satisfies the analytic formula $T_{566} = -\frac{3}{2}R_{56}$, yielding 54.9 mm in this case.

Implementation of the R_{56} optics will also require BPMs and steering correctors. These devices were not considered here, since they do not affect the optics, but it should be relatively straightforward to add them to the design.

3 Tuning Knob

Setting the R_{56} value in operation would benefit from a tuning knob, where the quadrupole and sextupole strengths (K_1 and K_2 values) in the R_{56} optics are programmed into the control software as analytic functions of the R_{56}. Hence, the magnet strengths can be quickly computed for any desired R_{56}. Typically, the tuning knob is based on an ideal optics, so it could be prepared in advance for use in operation. To make the knob, first, the optics is matched in MAD at a number of R_{56} points within the tuning range. Then the matched K-values for each magnet are fit to a polynomial function of the R_{56}. The resulting polynomials are used together as a knob for setting the magnet strengths at any desired R_{56} within the tuning range.

The polynomial functions must reproduce the input matched data very closely in order to minimize optics distortions due to unavoidable deviations between the fit and the exact K-values. Obtaining a good fit requires that the input matched K-values vary smoothly with the R_{56} to begin with. For this reason, the optics match in MAD is performed not only to produce the optimal optics functions, but also to make the R_{56} dependence of the matched K-values as smooth as possible. The latter is achieved by applying constraints on the variation of the matched K-values with the R_{56}.

As noted, the R_{56} tuning knob is designed based on the ideal lattice. However, it is expected to work reasonably well even in the operational lattice with errors. The reason is that the generated R_{56} and the first and the second order dispersion are local properties of the chicane, and hence, are not affected by the outside optics errors. The latter can only affect the chicane beta functions due to distortion of the incoming beta (BMAG). The only errors which can have an impact on the R_{56} are the errors of the chicane magnets (field, misalignment) which are expected to be small.

Figure 9 shows the matched K_1-values and the corresponding polynomial fit for the three families of the chicane quadrupoles within the R_{56} tuning range. Here, each quadrupole family consists of two quadrupoles positioned mirror symmetrically relative to the chicane center. The quadrupole field is within the magnet limit for the entire tuning range for beam energy exceeding 10 GeV.

Similarly, Figure 10 shows the matched K_1-values and the polynomial fit for the R_{56} matching quadrupoles located outside of the chicane. These include two existing LCLS-II quadrupoles (QBP28 and QBP35), and seven new quadrupoles (QBP37 to QBP43). They are arranged into eight families, where QBP35 and QBP43 are on the same string. The quadrupoles are within their field limit for up to 10 GeV.

Figure 11 shows the matched K_2-values and the polynomial fit for the chicane sextupoles. There are total of four sextupoles located mirror symmetrically relative to the chicane center, where a pair of sextupoles is placed next to each of the first and the last chicane quadrupoles. The four sextupoles of the LCLS-II type design provide the necessary strength for beam energy exceeding 10 GeV.

It should be noted that the chicane optics generates not only the desired first order term R_{56}, but also the second order term T_{566} and the higher order terms. Figure 12 shows the magnitude and variation of the chicane T_{566} versus the R_{56}. For typical operational values of particle momentum deviations δ, the effect of this T_{566} on the bunch longitudinal phase space should be small compared to the R_{56}.

Finally, Table 2 lists the polynomial functions for all the R_{56} magnet families; they make the complete tuning knob which could be implemented into the control software.

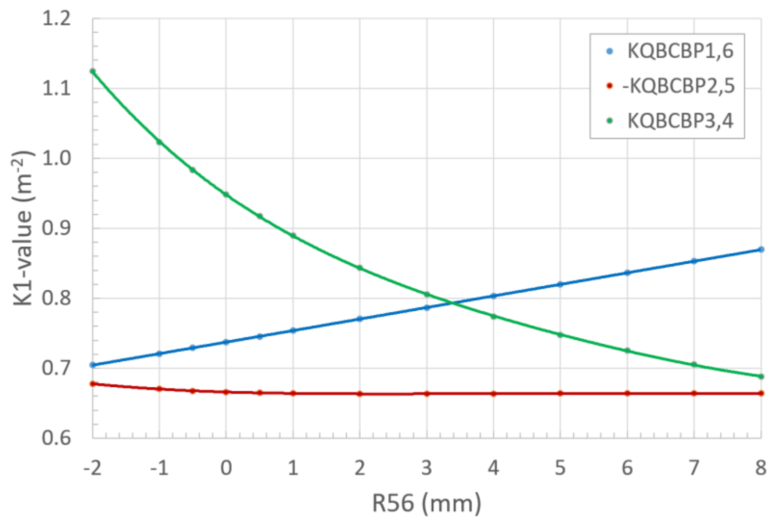

Figure 9: K_1-values of the three chicane quadrupole families versus R_{56}, where the circles represent the exact matched values, and the curves are the fitted polynomial functions. Each family consists of two quadrupoles located mirror symmetrically relative to the chicane center. The sign of the K_1-values for the family of QBCBP2 and QBCBP5 is reversed in this figure.

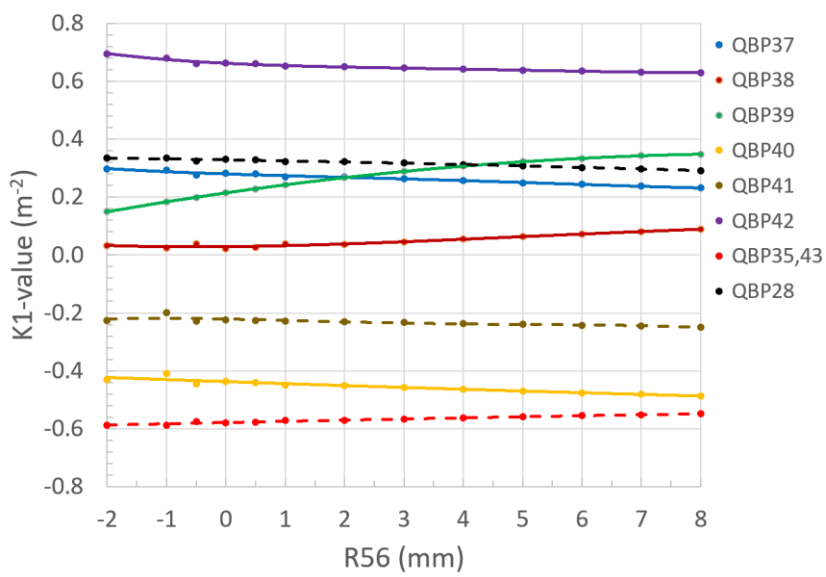

Figure 10: K_1-values of the eight matching quadrupole families versus R_{56}, where the circles represent the exact matched values, and the curves are the fitted polynomial functions.

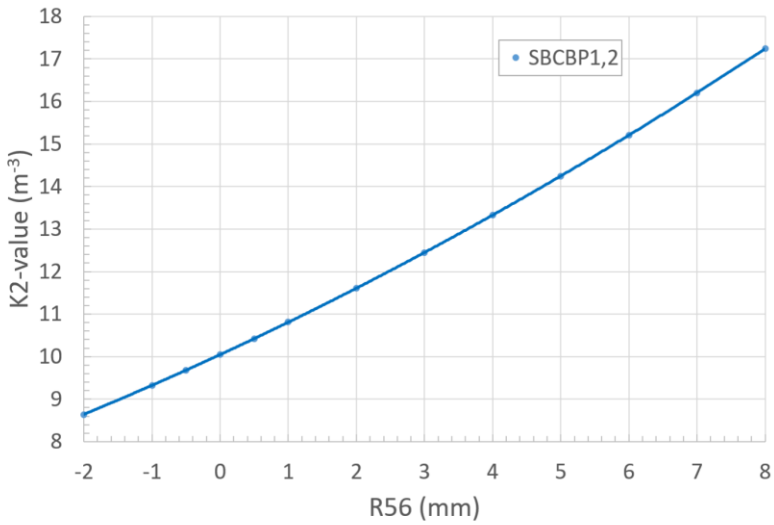

Figure 11: K_2-values of the chicane sextupoles versus R_{56}, where the circles represent the exact matched values, and the curves are the fitted polynomial functions. The four chicane sextupoles are located mirror symmetrically relative to the chicane center and have the same strengths (one family).

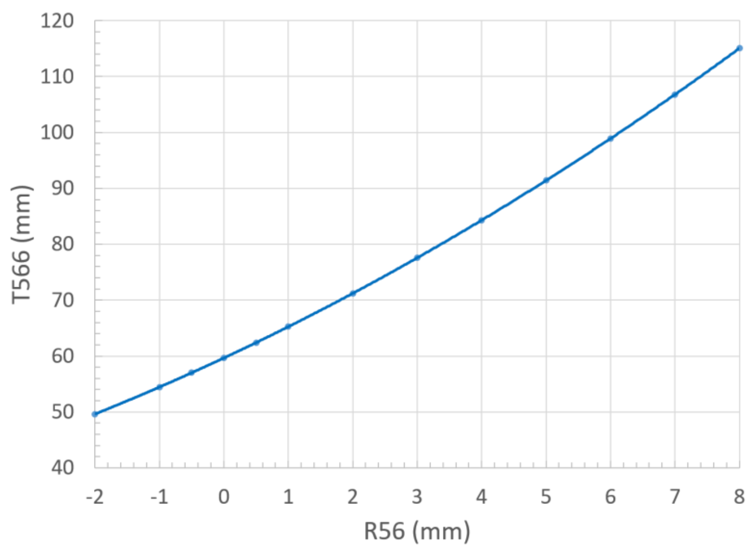

Figure 12: T_{566} generated in the chicane versus R_{56}.

Table 2: Polynomial fit of the quadrupole and sextupole K-values in the R_{56} optics, where x = R_{56} is in the range from -2 mm to +8 mm.

Chicane quadrupoles	
QBCBP1,6	K1 = 4.64073505E-06x^2 + 1.64762688E-02x + 7.37334224E-01
QBCBP2,5	K1 = -8.52872782E-06x^4 + 1.64804742E-04x^3 - 1.10848478E-03x^2 + 2.92104471E-03x - 6.66034035E-01
QBCBP3,4	K1 = 3.91478134E-05x^4 - 8.64249128E-04x^3 + 8.70229361E-03x^2 - 6.67585127E-02x + 9.47904091E-01
Bypass matching quadrupoles	
QBP37	K1 = 1.22191715E-05x^4 - 1.86271203E-04x^3 + 7.95595070E-04x^2 - 6.76682392E-03x + 2.79968792E-01
QBP38	K1 = 4.74849053E-06x^4 - 1.60708019E-04x^3 + 1.68522978E-03x^2 + 1.91029303E-03x + 2.88070849E-02
QBP39	K1 = -1.59128961E-03x^2 + 2.94488927E-02x + 2.14445838E-01
QBP40	K1 = 9.80757596E-05x^2 - 6.99328796E-03x - 4.37143619E-01
QBP41	K1 = -2.93654830E-05x^4 + 3.82043658E-04x^3 - 1.15408606E-03x^2 - 3.86236661E-03x - 2.21049419E-01
QBP42	K1 = 2.35447824E-05x^4 - 4.06812497E-04x^3 + 2.51309950E-03x^2 - 1.01067939E-02x + 6.62053109E-01
QBP35*,43	K1 = -6.21895988E-05x^2 + 4.29427860E-03x - 5.78488626E-01
QBP28*	K1 = -1.50780460E-04x^2 - 3.43648299E-03x + 3.28655210E-01
Chicane sextupoles	
SBCBP1,2	K2 = 1.97783735E-02x^2 + 7.41263213E-01x + 1.00482905E+01

* Existing LCLS-II quadrupoles

4 Summary

A dedicated optics is designed for R_{56} tuning in the LCLS-II. The optics consists of a four-dipole chicane with inner quadrupoles and sextupoles for R_{56} tuning and up to second order dispersion cancellation, as well as quadrupoles outside of the chicane for matching the beta functions. For a cost-effective solution, the optics design is based on the LCLS-II type magnets, and it does not require changes to the existing LCLS-II magnet layout. The optics is inserted at end of the LCLS-II bypass beamline, where sufficient free space is available. Since this location is upstream of the beam spreader, the R_{56} tuning affects bunches going to either undulator. The optics provides the R_{56} tuning range from -2 mm to +8 mm for beam energy up to 8.5 GeV. A tuning knob, based on polynomial fit of the quadrupole and sextupole K-values as a function of R_{56} is created, which can be used in operation for setting the magnet strengths.

5 Acknowledgements

This work is performed as part of the LCLS-II beam shaping study at SLAC. We thank Agostino Marinelli, Yuantao Ding, and Zhirong Huang for proposing the R_{56} optics study and helpful discussions. The work is supported by the U.S. DOE Contract DE-AC02-76SF00515.

6 References

[1] H. Grote and F. C. Iselin, "The MAD Program," http://mad8.web.cern.ch/mad8/.

[2] T. O. Raubenheimer, "LCLS-II: status of the CW X-ray FEL upgrade to the SLAC LCLS facility," Proc. 37th Int. Free Electron Laser Conf. (FEL'15), WEP014, Daejeon, Korea, 2015.

[3] "Injector Laser Heater Requirements," LCLSII-2.2-PR-0086.

[4] "BC1 Bunch Compressor Chicane Requirements," LCLSII-2.4-PR-0039.

[5] "BC2 Bunch Compressor Chicane Requirements," LCLSII-2.4-PR-0040.

[6] "R56 Compensation Chicanes," LCLSII-2.4-PR-0447.

[7] J. Qiang, et al, "Design Optimization of Compensation Chicanes in the LCLS-II Transport Lines," Proceedings of IPAC2016, TUPOR018, Busan, Korea, 2016.

[8] A. Marinelli and Y. Ding, private communication.

[9] "LCLS-II-HE Beam Stay Clear PRD," LCLSII-HE-1.3-PR-0129.